Ukrainian Journal of
Veterinary and Agricultural Sciences
http://ujvas.com.ua

Stepan Gzhytskyi National University of Veterinary Medicine and Biotechnologies Lviv

original article | UDC 544.723 | doi: 10.32718/ujvas3-2.03

Volume 3
Number 2

Removal of Cd^{2+} from aqueous solution by zeolite synthesized from Egyptian kaolin

Asmaa Kamel Bahgaat[1*], Helmy El-Sayed Hassan[2], Ahmed Abddel Aziz Melegy[3], Ahmed Mohamed Abd-El kareem[1], Manar Hassan Mohamed[2]

[1]*Soil Chemistry Dept. Desert Research Center (DRC), Cairo, Egypt*
[2]*Laser Application in Metrology, Photochemistry and Agriculture Dept., National Institute of Laser Enhanced Sciences (NILES), Cairo University*
[3]*Geological Sciences Dept., National Research Center (NRC), Giza, Egypt*

Article info
Received 24.03.2020
Received in revised form 27.04.2020
Accepted 28.04.2020

Correspondence author
Asmaa Kamel Bahgaat
E-mail: akbahgaat@hotmail.com

Abstract

Zeolite Na-Y was prepared from kaolin located in Wadi-Hagul, Suez, Egypt. The synthetic zeolite prepared by the hydrothermal reaction of kaolin was characterized by X-ray fluorescence (XRF), X-ray diffraction (XRD), scanning electron microscopy (SEM) and cation exchange capacity (CEC). Cadmium ion removal was investigated using the synthetic solution of Cd^{2+} ions with different concentrations at room temperature (25 °C ± 0.2), initial pH of the solution and contact times. The optimum contact time for removal of Cd^{2+} ion was 10 min, with 0.1g of synthetic zeolite and pH 7.57. The experimental data were correlated using Langmuir, Freundlich and Harkins-Jura adsorption isotherms. The maximum adsorption capacity Q_m obtained from the Langmuir isotherm was 14.006 mg/g for Cd^{2+} ion. Kinetic studies reveal that synthetic zeolite is more effective as adsorbent for removing cadmium ions.

Key words: Egyptian synthetic zeolite-Y, Adsorption isotherms, Kinetic models, Cd^{2+}, Removal, Distribution coefficient.

Citation:
Asmaa Kamel Bahgaat, Helmy El-Sayed Hassan, Ahmed Abddel Aziz Melegy, Ahmed Mohamed Abd-El kareem, & Manar Hassan Mohamed (2020). Removal of Cd^{2+} from aqueous solution by zeolite synthesized from Egyptian kaolin. *Ukrainian Journal of Veterinary and Agricultural Sciences*, 3(2), 12–23.

1. Introduction

Heavy metal pollution seriously harms the environment and human health resulting in reduced growth and development, as well as diseases such as cancer, organ and nervous system damage, along with the ecosystem (Yuna, 2016; Hong et al., 2019). Environmental pollution became one of the common important subjects that attract the attention of many scientists at present (Fathy et al., 2016). The removal of heavy metals (Pb^{2+}, Zn^{2+}, Cd^{2+}, $Cu^{2+}$and Cr^{2+}) from wastewater has been received great attention, because of the adverse effect on the health and the natural environment (Ismael et al., 2012; Merrikhpour & Jalali, 2013; Guan et al., 2019).Various treatment processes are available, among which ion-exchange is considered to be cost-effective if low-cost ion-exchangers such as zeolites are used (El-Naggar et al., 2019).

The use of alternative low-cost materials with high selectivity as potential sorbents has been emphasized recently (Ji et al., 2020).

Adsorption is a special characteristic of zeolites which is usually ion exchange occurs into the pore openings of the ion exchanger and active side on the surface. The amount of metal ion to be adsorbed is strongly affected by the nature and concentration of the metal ion, pH, and metal solubility, presence of competing and complexion ions (El-Naggar et al., 2019).

Natural kaolin is the most common clay mineral of a group of hydrous aluminum silicate, has a typical 1 : 1 layered structure, with one tetrahedral and one octahedral sheet,

which results from the breaking of aluminum-rich silicate rock, such as feldspar (Aveen & Kafia, 2014; Aragaw & Ayalew, 2018). Thus, Kaolinite mineral can be a potential adsorbent owing to its low cost, rich natural abundance, and high mechanical and chemical stability.

Zeolite NaY is a material with regular architecture and micropores consist of cavities and channels. Zeolite NaY is a material with regular architecture and micropores consist of cavities and channels. Zeolite NaY has a wider application as catalyst and adsorption (Ayoola et al., 2017; Warzybok & Warchol, 2018).

Zeolites have satisfactory capacity adsorption for heavy metals removal due to their high cation exchange capacity and surface sorption properties (Aragaw & Ayalew, 2019; Guan et al., 2019). The exchangeable cation (sodium, potassium, or calcium) balances the net negative charge. These cations are exchangeable with certain cations in solutions such as lead, cadmium, zinc, and manganese.

However, synthetic Zeolites are preferred for industrial applications, such as adsorption, catalysis, and ion exchange, then their natural counterparts due to more uniform pore sizes, relative ease of manufacture, low costs and can be tailored to specific shape and size needs. Many synthetic molecular sieves have a pore size range of 3.5–4.5Å for zeolite LTA (Z–A), 4.5–6.0 Å for ZSM-5 and 6.0–8.0 Å for zeolite X and Y (Khalifah et al., 2018).

The objective of this study is to prepared synthetic zeolite-Y from Egyptian kaolin, Wadi Hagul area and to investigate the capacity and performance of synthetic zeolite-Y for removal of Cd^{2+} from prepared solution.

2. Materials and methods

Preparation of (Synthesis Zeolite Na-Y) from Egyptian kaolin

Prepared samples

Raw representative sample of natural, poorly crystalline clay mineral (kaolin) was collected from Wadi-Hagul, Suez, Egypt. The location of the study area (Latitude 29° 44' 13.5" N and longitude 32° 14' 08.2" E) is shown in (Fig. l). Clay samples were air dried at 80 °C and grinded to fine powder by using standard sieves to obtain the fine powder less than (40 µm) (Black et al., 1985).

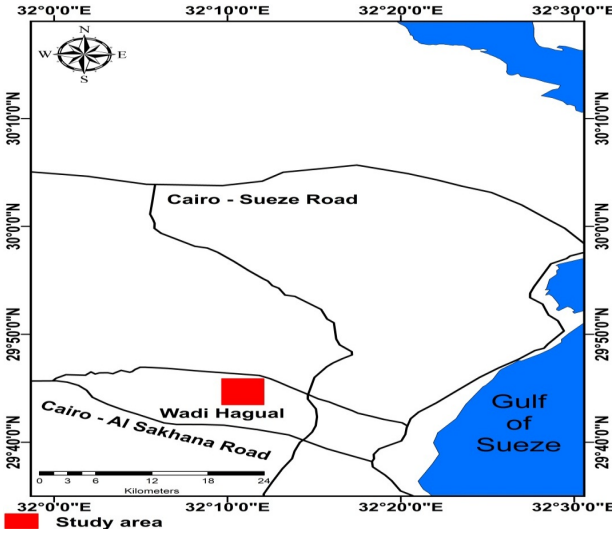

Fig. 1. Location of raw material (kaolin) in Wadi Hagul, Suez, Egypt

Hydrothermal synthesis

Calcined of natural Egyptian Kaolin (NEK) for 6 h at 800 °C. Through this process kaolin converted into metakaolinite phase (Rahman et al., 2018; Warzybok & Warchoł, 2018). Metakaolinite was mixed with (1.0 M Na OH) solution and used as starting material without any additional silica to the reaction mixture. Na OH was utilized as homogeneous catalyst which is a nonrenewable and becomes consumable chemical in the process (Fatimah & Rubiyanto, 2018). The solid/liquid ratio of metakaolinite to alkaline solution was (10 g/100 mL) in covered Teflon cups. The suspension was stirred at 800 rpm at room temperature for 24 h to obtain a homogenous fusion of solid as presented in (Adeoye et al., 2017). The slurry was transformed to the dry oven for treatment at 90 °C/2d under ambient pressure to synthesize zeolite-Y according to (Tavasoli et al., 2014; Ayoola et al., 2018; Olaremu et al., 2018). The residue product was filtered and washed till (pH less than 8). The residue was dried overnight at 100 °C. The steps of synthesis zeolite are shown in (Fig. 2). The high crystallinity product zeolite-Y and the raw material are characterized by XRF, XRD, and SEM (Somderama et al., 2019).

Characterization of synthetic zeolite and kaolin

Chemical and mineralogical composition of raw material (kaolin), metakaolin, final zeolite-Y product were determined by X-ray fluorescence (XRF) instrument model AXIOS, WD-XRF Sequential Spectrometer (for the elemental composition) (Iftitahiyah et al., 2018). X-ray diffraction analysis (XRD) was applied using an Empyrean PANalytical diffractometer with Cu, Kα radiation at 40 kV with the current 30 mA. The diffractograms were recorded in 0.0263°2θ. The diffraction data were analyzed of both the kaolinite and the resulting zeolite product and the morphology was examined using scanning electron microscope (SEM). The scanning electron microscope using SEM Model Quanta 250 FEG (Field Emission Gun) attached with EDX Unit (Energy Dispersive X-ray Analyses), with accelerating voltage 30 K.V., magnification14x up to 1000000 and resolution for Gun.1n.

pH and EC were determined in both aqueous solution and clay minerals by glass electrode and electrical conductivity respectively. Cation exchange capacity (CEC) is measured by the sodium saturation method are shown in Table 2.

Table 1
Chemical composition and physical composition of natural Egyptian kaolin, metakaolinite and synthesis zeolite-Y (wt. %)

Main constituents	Clay mineral (Kaolin)	Metakaolinite	Synthesis zeolite-Y
	(wt %)	(wt. %)	(wt %)
SiO_2	48.58	55.93	39.46
TiO_2	2.77	1.33	1.46
Al_2O_3	19.96	24.47	17.68
$Fe_2O_3^{tot.}$	16.10	10.92	13.80
MnO	0.04	2.11	0.02
MgO	0.64	N.D	1.41
CaO	1.33	1.03	0.86
Na_2O	0.08	1.26	7.79
K_2O	0.88	0.67	0.53
P_2O_5	< 0.01	0.09	0.05
Cl	0.51	0.07	0.04
SO_3	0.03	0.01	0.02
L.O.I.*	8.84	1.90	16.59

*L.O.I: Loss on ignition

Table 2
Chemical characteristics of the studied materials

Materials	pH 17.5 ± 0.5 °C	CEC* (meq/100g clay)	EC* ds/m
Synthesis zeolite-Y (SEZ)	10.23	401.09	0.949
Kaolin (EK)	8.18	50.30	8.88

*CEC: Cation exchange capacity.
*EC: Electrical conductivity

The total cation exchange capacity (CEC) of zeolite-Y and kaolin is the amount of all exchangeable cations and it is defined by the number of equivalents of fixed negative charges per amount of zeolite (Yusof et al., 2010).

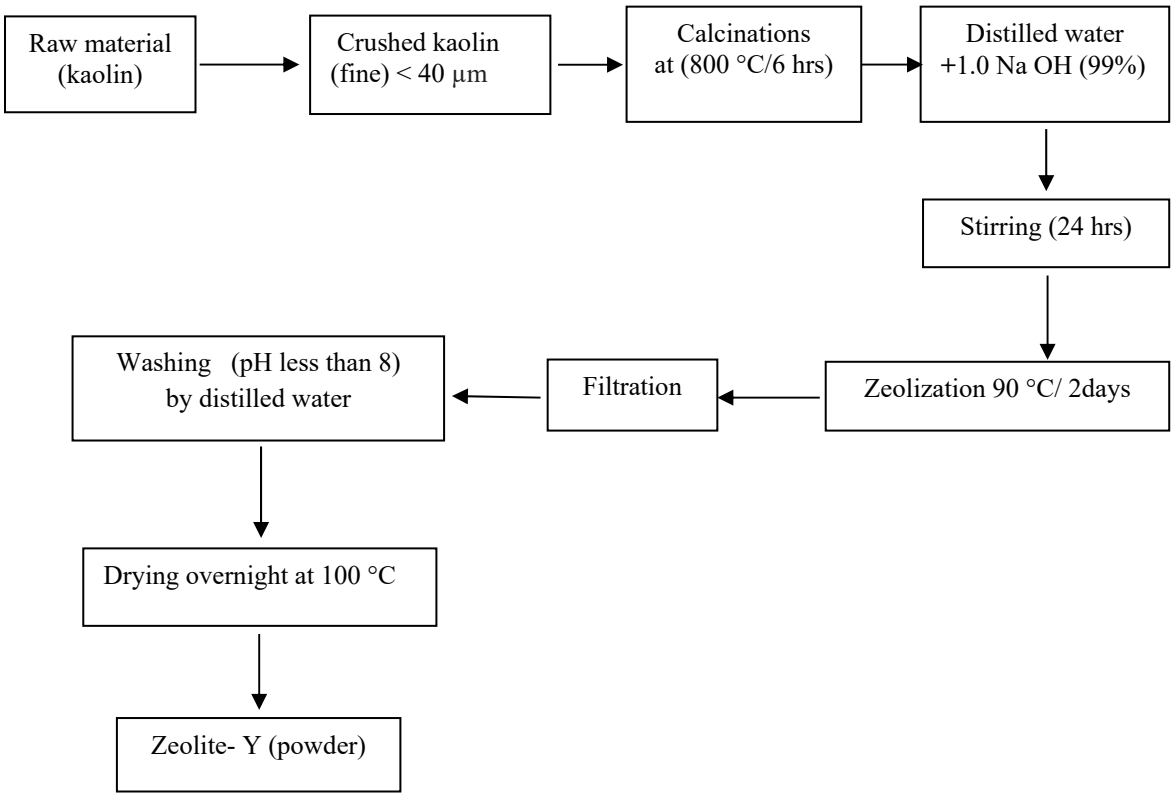

Fig. 2. Schematic diagram for the preparation of zeolite-Y from kaolin

Batch Adsorption Experiments

Heavy metal ions removal was determined in terms of initial concentration, pH, and contact time. A stock solution of concentration 1000 mg/L from Cd^{2+} solution was prepared by dissolving an appropriate amount of $Cd(NO_3)2.4H_2O$, diluted in deionized distilled water (DDW). Solution ionic strength was controlled by adding a 50 mL of 0.05 M KNO_3, background electrolyte solution containing different concentrations of Cd^{2+} ions (10, 15, 20, 25 and 30 mg/L). In the study of the impact of contact time, 0.1 g of synthetic zeolite (SEZ) mixed with 50 mL of the 10 mg/L of Cd^{2+} solution at 5, 10, 20, 40, 60, 80,100, 120 and 180 min (Jamil et al., 2010) to establish the ability of synthetic zeolite to retained Cd^{2+} ions (to determine the suitable time to adsorb the metal from the waste solution by synthetic zeolite). Supernatant aliquots were filtered through Whatman filter paper (No. 42) (particle retention 2.5 mL) before chemical analysis. The pH of the solution was measured before and after treatments, pH of initial solutions before the addition of adsorbent was determined 5.95. In these experiments, these solutions are simulated in terms of the pH of real wastewater. The concentrations of metal ions in the solutions before and after adsorption were determined using Inductively Coupled Plasma (ICP) 6500 Duo, Thermo Scientific, England.1000mg/L multi-elements certified standard solution; Merck, Germany).

For studying the influence of the different concentrations, 0.1g from SEZ and 50, mL of heavy metal solution in the concentration range (10–30 mg/L) (EL Zayat, 2014). The suspensions were shaken at 350 rpm on a reciprocating shaker at room temperature (25 ± 0.2 °C). After equilibration at the contact time, the supernatants were separated by centrifugation at 3000 rpm/10 min (RoTofix 32A ttettich ZentRifugen RPMx RcFx100) and filtered through a Whatman filter paper (No. 42) (particle retention 2.5 lm). The amount of metal removed from the solution was taken as the difference in concentration between the amount added initially and that remaining in solution after equilibration (Chen et al., 2011).

The removal efficiency (%) adsorption capacity (q_e) was calculated using the equation (1) and equation (2), respectively (Franus et al., 2019; Rahimi & Mahmoudi, 2020):

Removal efficiency

$$\% = \frac{(C_\circ - C_e)}{C_\circ} * 100 \quad (1)$$

Adsorption capacity

$$q_e(mg/g) = \frac{(C_\circ - C_e) * V}{m} \quad (2)$$

where: q_e is the equilibrium adsorption capacity of the adsorbent (mg/g), that is the amount of adsorbed metals was taken as the difference in concentration between the amount added initially and that remaining in solution after equilibra-

tion (Oren & Kaya, 2006; Hong et al., 2019), C_o and C_e are the initial and remaining concentrations of the heavy metal in the liquid phase (mg/L) at time t, V is the volume of aqueous solutions (L), and m is the mass of the adsorbent (g).

The distribution coefficient (binding energy) K_d has been used to indicate the adsorption affinity of a solid adsorbent toward a solute (Naiya et al., 2009). Was obtained from the following equation:

$$K_{d\,(}mL/g) = \frac{(C_o - C_e)}{C_e} * \frac{V}{m} \qquad 3$$

where C_e (mg/L) is the equilibrium concentration of Cd^{2+}ions.

3. Results and discussion

Zeolite and kaolin characterization

Chemical properties

From Table 1, zeolite and kaolin vary in the alkalinity degree. Synthetic zeolite-Y and kaolin showed higher alkalinity (pH 10.23 and 8.18), respectively. The materials salinity was noticed with different degrees, kaolin is moderately saline and synthetic zeolite-Y is non-saline (Hardie & Doyle, 2012).

The cation exchange capacity (CEC) results revealed that the obtained CEC for synthetic zeolite-Y was higher than kaolin 401.09 meq/100g clay and 50.30 meq/100g clay, respectively.

Chemical and mineralogical analysis

The chemical composition (in wt. %) of kaolin before and after calcination and synthesis zeolite was listed in Table 1. The synthesis zeolite from kaolin formed in two steps, the first step is the metakaoliniziation and the second is zeolization. The volatile matter of the clay developed and di hydroxylation takes place in the course of calcination at 800 °C/6 h. The X-ray pattern of (unheated) kaolin is shown in (Figure 3a), the XRD pattern of raw material (kaolin) it contains kaolinite (K), Na-montmorillonite (Mo) and quartz as major impurities (Qz). The metakaolinization of kaolin by heating for 6 h at 800 °C resembled all the kaolinite peaks expect for the peaks due to the admixed impurities. Figure 2b shows that the characteristic peaks of kaolinite disappear during the calcination step and reduce in peaks intensity of quartz. The crystallinity of the zeolite-Y increase with increasing the time at 2d of metakaolinite. Na OH (1.0 M) at 90 °C/2d) used to produce the synthetic zeolite-Y. Figure 3c shows the peaks of zeolite-Y with small peaks of zeolite-P. The zeolite Y in pure phase was crystallized at 90 °C at a time of crystallization of 48 hours, and this result is agreement with (Ayoola et al., 2017; Belaabed et al., 2017). Zeolites formation was observed in (Figure 4c). The chemical formula of

zeolite Na-Y is: $Na_{60}\ H_{32}\ (Si_{100}\ Al_{92}\ O_{384})$

zeolite- P is: $Na_6\ Al_6\ Si_{10}\ O_{32} \cdot 12\ H_2O$

Figure 4 shows (SEM) micrographs of raw material (4a), metakaolinite under hydrothermal conditions with Na OH (4b) and synthetic zeolite –Y (4c).

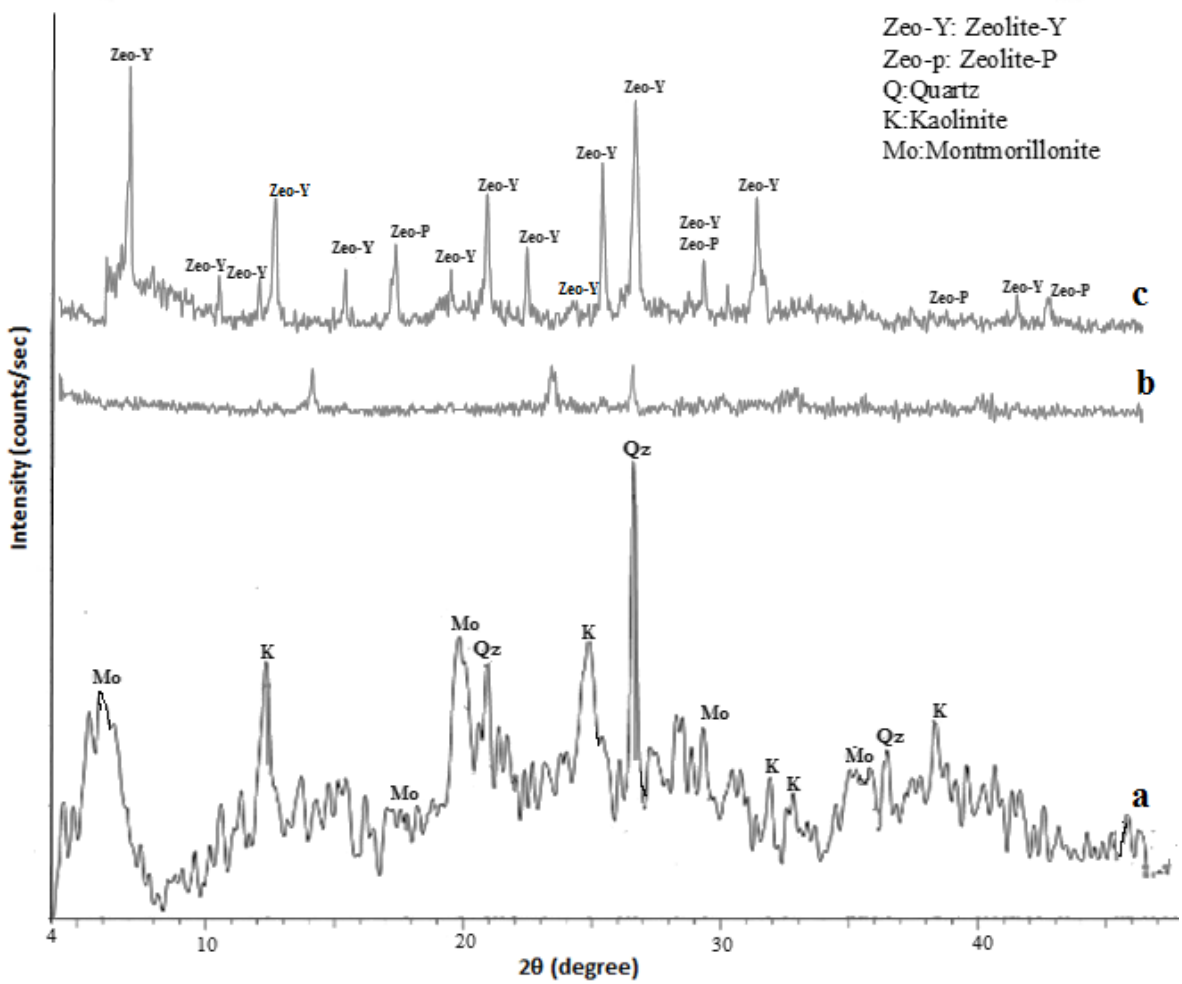

Fig. 3. XRD pattern of raw material (kaolin) (a), metakaolinte (b) and synthetic zeolite –Y (Zeo-Y) (c).

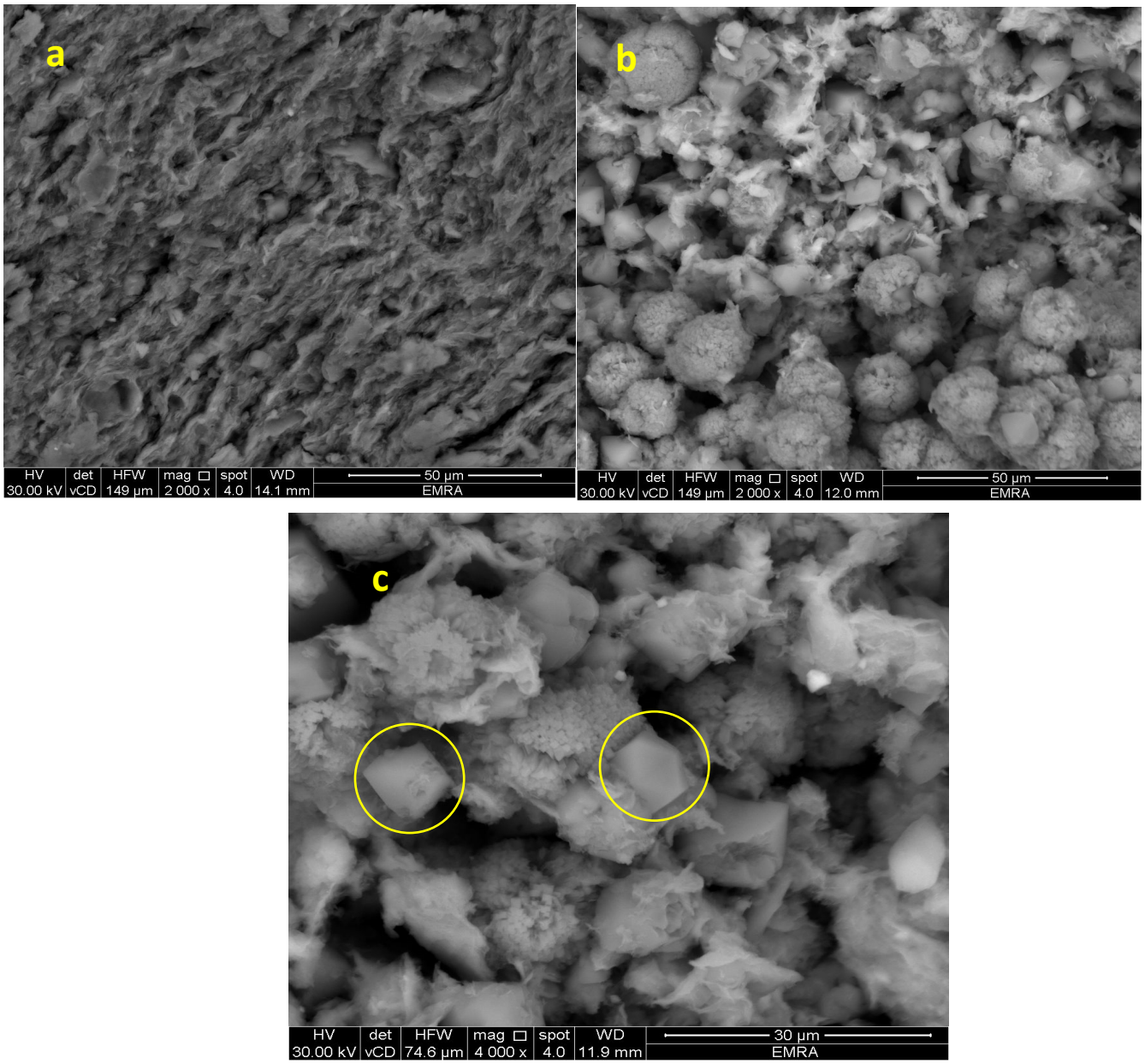

Fig. 4. SEM micrographs of the prepared zeolite from kaolin raw material (a), metakolinte under hydrothermal conditions with Na OH (1.0M) / 90ºC /2days (b) and synthetic zeolite Na-Y (octahedral structure) (c).

Efficiency of synthetic zeolite for removing Cd^{2+} ions

Zeolites were characterized by their higher capabilities for removing heavy metal ions because of their large specific surface area, channels and cavities, and their high number of negatively charged bonding sites. Besides, their ability to close fissures and cracks, which may form paths for leachates.

Optimum contact time

The results of the optimum contact time were given in Figure 4 of the removal efficiency of Cd^{2+} ions using zeolite-y at room temperature. It was noted that the maximum amount adsorbed (q_t mg/g) on synthetic zeolite was fast in the first 10 minutes and the percentage of removal efficiency reached 99.93 % as shown in Figure 6**.** The fast adsorption at the initial uptake was probably due to the interaction between Cd^{2+} ions (adsorbate) in the solution and active sites those available on the zeolite-y (adsorbent) surface take place. The equilibrium of adsorption occurs when all active sites on the surface of Zeolite were blocked by Cd^{2+} ions from the solution (Mehdizadeh et al., 2014). This may be attributed to the fact that SEZ can act as an ion exchanger. The adsorption capacity depends on the dose of adsorbents, contact time and pH (Jamil et al., 2010).

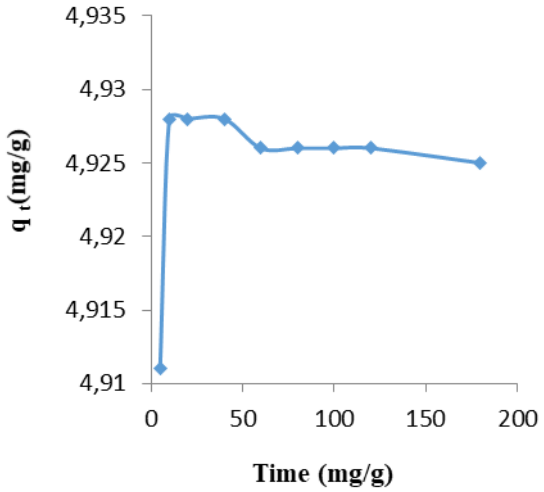

Fig. 5. The adsorbed amount (q_t) of Cd^{2+} ions were removal adsorbed onto SEZ at 10 mg/L of Cd^{2+} (25± 0.2°C)

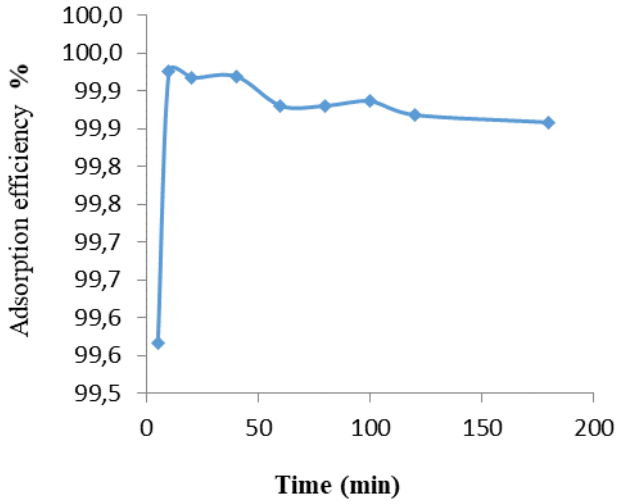

Fig. 6. Effect of contact time on the efficiency of SEZ

Adsorption kinetic studies

To design a convenient adsorption process, one should have enough information about the rate at which adsorption occurs. Thus, the rate of constants for the adsorption of Cd^{2+} ions from aqueous solution onto SEZ was determined in Figure 6 using the three kinetic models. They can be used for examination of the controlling mechanisms of the adsorption process, such as chemical reaction, diffusion control, and mass transfer onto an adsorbents namely pseudo-first-order, pseudo-second-order and Intra-particle diffusion kinetic models (equations 3, 4 and 5) (Yildiz, 2017; Franus, et al., 2019; Kwakye-Awuah et al., 2019). The comparison between the three kinetic models are presented in Table 3. The theoretical $q_{e\text{-}cal}$ values calculated by the pseudo-second-order model were found to closer to the experimental $q_{e\text{-}exp}$ values and the correlation coefficients R^2 were higher for the Cd^{2+} ion. Therefore, the second-order kinetics model described the adsorption of Cd^{2+} ions onto synthetic zeolite.

Pseudo-first-order equation (PFO)

The pseudo-first-order equation was represented by the following equation (Lagergren, 1898)

$$\text{Log}\,(q_e - q_t) = \log q_e - [(k_1/(2.303)*t] \qquad (3)$$

where: q_e and q_t (mg/g) are the concentration of metal ions in the adsorbent at equilibrium and at time t respectively, and k_1 is the pseudo-first-order rate constant (min^{-1}) k_1 and $q_{e\text{-}cal}$ can be determined from the slope and intercept of the linear plot of $\log(q_e - q_t)$ versus t as Figure 7.

Pseudo-second-order equation (PSO)

To model the sorption kinetics, a pseudo-second-order rate equation was employed (Ho & McKay, 1998). The pseudo-second-order rate equation was represented as:

$$t / q_t = 1 /(k_2 q_e^2) + (1 / q_e)\, t \qquad (4)$$

where k_2 is the rate constant of the pseudo-second-order equation, q_t (mg/g) is the amount of Cd^{2+} sorbed on different adsorbents materials at time t (min) and q_e is the equilibrium sorption capacity (mg/g). k_2 and theoretical $q_{e\text{-}cal}$ values were obtained from the intercept and slope of the plot of t/q_t versus t as Figure 8.

And the initial sorption rate h at various initial concentrations is related in the following equation

$$h = k_2 q_e^2 \qquad (5)$$

where: h (mg / g min) is the initial sorption rate.

Intra-particle diffusion model (IPD)

The diffusion model analysis can be represented using the intra-particle model. This kinetic model was proposed by (Zewail & Yousef, 2015; Ali, 2018). The linearize equation is expressed as in equation (6).

$$q_t = K_{id} \cdot t^{0.5} + C \qquad (6)$$

where: K_{id} denotes a constant of intra- particle diffusion ($mg/(g \cdot min^{0.5})$), $t^{0.5}$ is the square root of the time and C (mg/g) is the intercept relative to the thickness of the boundary layer (Fakhri, 2017).When q_t versus $t^{0.5}$ as Figure 8, the graph is plotted, the linearity of the curve indicates that intra-particle diffusion takes place within the bio-sorption system. The main rate-limiting step for the adsorption was the intraparticle diffusion process. On the other hand, if the relationship q_t vs. $t^{0.5}$ does not pass through the origin or is non-linear, the adsorption process is accompanied by other mechanisms (Franus, et al., 2019; Kwakye-Awuah et al., 2019).

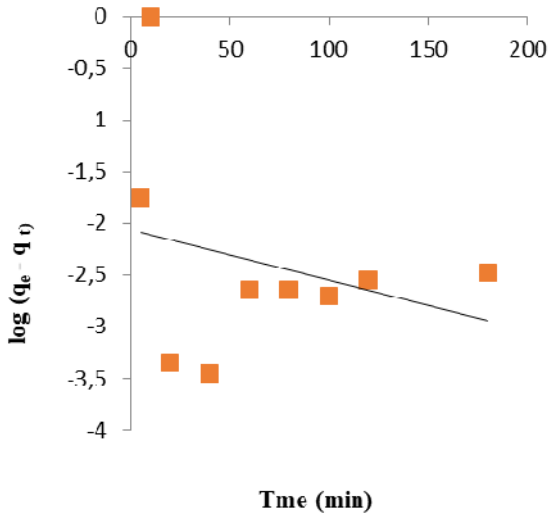

Fig. 7. Pseudo-first-order kinetic modeling of Cd^{2+} adsorption onto SEZ at initial concentration 10 mg/L (25 ± 0.2 °C)

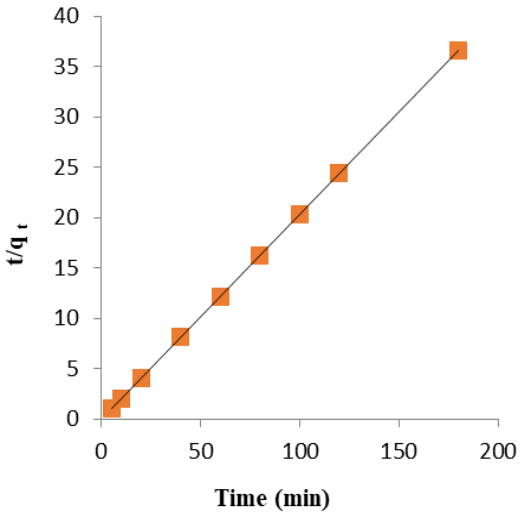

Fig. 8. Pseudo- second-order kinetic modeling of Cd^{2+} adsorption onto SEZ at initial concentration 10 mg/L (25 ± 0.2 °C)

Figure 8 shows that the plot of t/q_t versus t is a straight line. The values of qe and intercept k_2 were calculated from the slope and intercept and were tabulated in Table 3. The experimentally obtained $q_{e\text{- exp}}$ value was found to be in good agreement with the $q_{e\text{-cal}}$ values calculated from kinetic experiments (Chen & Shi, 2017; Fakhri, 2017). According to the (PSO) model, high correlation coefficients (R^2) for 10 mg/L of Cd^{2+} (R^2 = 1.00) onto SEZ. These results suggested that the sorption kinetics of Cd^{2+} onto SEZ adsorbent follows a PSO process and that the overall rate constant of Cd^{2+} ion was controlled by the chemisorption process (Fahmy et al., 2016).

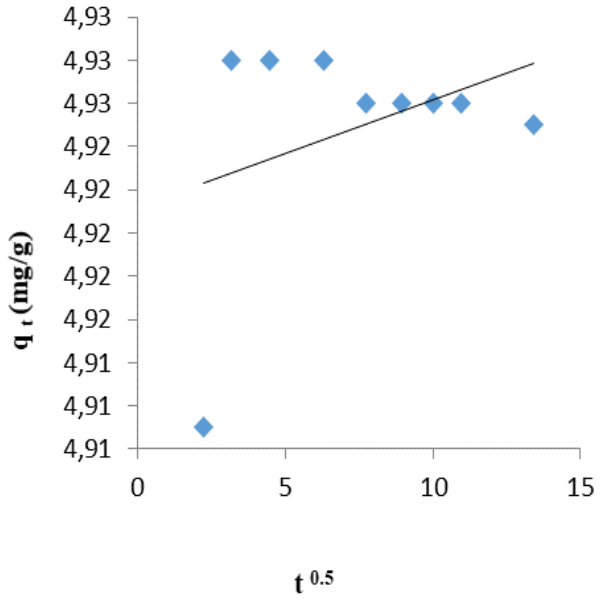

Fig. 9. Intra- particle diffusion kinetic modeling of Cd^{2+} adsorption onto SEZ at initial concentration 10 mg/L (25 ± 0.2 °C)

Table 3
Kinetic parameters for pseudo-first, second-order and intra-particle diffusion adsorption kinetic models of Cd^{2+} ions sorption onto SEZ

Kinetic Models	Parameter	Adsorbent Synthetic zeolite-Y
Pseudo-first order		
	$q_{e,\text{-exp}}$ (mg/g)	4.928
	$q_{e,calc}$ (mg/g)	0.0087
	K_1	0.011
	R^2	0.077
Pseudo-second order		
	$q_{e\text{-},calc}$ (mg/g)	4.926
	K_2 (g/mg min)	24.24
	h (mg/g min)	588.24
	R^2	1
Intra-particle diffusion		
	k_{id} (mg/g $min^{0.5}$)	0.0005
	Intercept (C_i)	4.921
	R^2	0.122

Adsorption Studies

Cadmium Sorption Behavior

Adsorption isotherms were presented in Figure 10. The amount of adsorbed metals increased with an increase in the initial adsorbate concentration from 10 to 30 mg/L. The maximum adsorption capacity value of Cd^{2+} obtained from the Langmuir equation. Table 4 shows the maximum sorption capacity (Q_m) which represents monolayer coverage of sorbent with sorbate as shown in Figure 10. According to (Naiya et al., 2009) at lower concentrations, all of the Cd^{2+} ion in the solution would interact with the binding sites and it was favor almost 100 % adsorption. At higher concentrations, more Cd^{2+} ions were left un-adsorbed in the solution. The Cd^{2+} ion adsorption was referring to different mechanisms of ion exchange as well as to the adsorption process. During the ion exchange process, the Cd^{2+} ion had to be moved through the pores of the adsorbent mass, but also through the channels of the lattice, they have to be replaced exchangeable cations due to the saturation of the binding sites. It was observed that adsorption onto this material is

practically linear in solutions containing one metal (Mishra & Patel, 2009).

Figure 11 shows that the free adsorption sites reduced by increasing the initial concentration of Cd^{2+} ions, therefore, the best initial concentration of solid adsorbents was 10mg/L, this is consistent with (Naiya et al., 2009; Chen et al., 2011; Al-Rudaini, 2017).

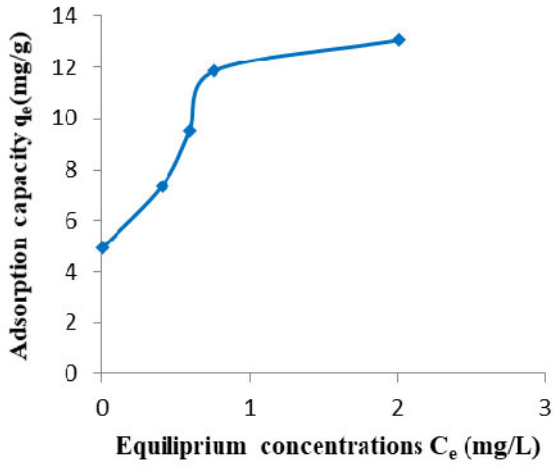

Fig. 10. Adsorption capacity of Cd^{2+}onto SEZ

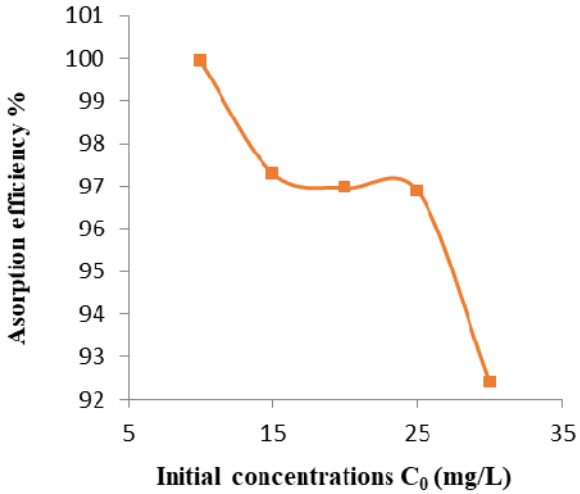

Fig. 11. Effect of initial concentration on removal efficiency percentage of SEZ

K_d in Figure 12 represents the function of Cd^{2+} ions concentration. The values of distribution coefficient (binding energy) K_d was calculated by equation (3) and decreased with the increasing concentration of Cd^{2+} ions. All of the Cd^{2+} ions in the solution will interact with the binding sites at lower concentrations and thus facilitate more than 95 % adsorption (Shaheen et al., 2012). At high concentrations, due to the saturation of the binding sites ions were left unabsorbed in the solution. This indicates that the energetically less favorable sites become involved with increasing ion concentration in aqueous solution. The Cd^{2+} ions adsorption was attributed to different mechanisms of ion exchange as well as to the adsorption process. During the ion exchange process, the Cd^{2+} ions had to be moved through the pores of the adsorbent mass, but also through the channels of the lattice, they have to be replaced exchangeable cations (Naiya et al., 2009).

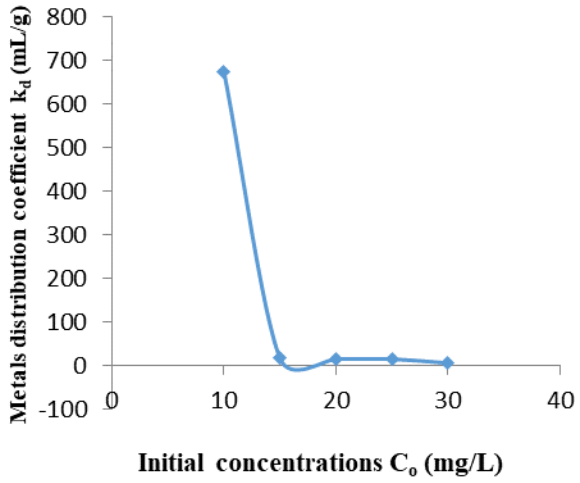

Fig. 12. Effect of initial concentration on the K_d of Cd^{2+} ions onto SEZ

Adsorption isotherms

The adsorption isotherms are very important for describing the adsorption mechanism of metal ions onto the adsorbent and plays an important role in the identification and evaluation of the maximum capacity onto adsorbents, three adsorption isotherms models namely Langmuir, Freundlich and Harkins-Jura isotherms models (Yuna, 2016; Erdogan, 2019). For Langmuir adsorption isotherm model is an example of a favorable isotherm and is applicable under an assumption: a uniform surface of the solid, the absence of interaction between the different adsorbed molecules, adsorption in a monolayer and adsorption occurs on a structurally homogeneous adsorbent (Mishra & Patel, 2009). This model is presented by equation (7) (Langmuir, 1918).

Langmuir adsorption isotherm

$$q_e = Q_m k_L C_e/(1+k_L C_e) \quad (7)$$

where: q_e (mg/g) is the adsorbed amount of metal ions, $C_{e\ (mg/L)}$ is the equilibrium concentration of metal ions in the solution, Q_m is the monolayer adsorption capacity, is the amount of metal ions at complete monolayer coverage (mg/g), K_L is the energy of sorption constant. The linear form of Langmuir isotherm equation (8) is given by:

$$C_e/q_e = (1/(K_L Q_m)) + (C_e/Q_m) \quad (8)$$

The Langmuir parameters can be used to predict the affinity between the sorbate and the sorbent using the dimensionless separation factor R_L (Rani & Sasidhar, 2012; Aly et al., 2014; Franus et al., 2019).

$$R_L = 1/(1+(k_L * C_o)) \quad (9)$$

where: C_o the initial concentration (mg/L) of Cd^{2+}, k_L is the dimensionless Langmuir parameter constant (L/mg). The value of the equilibrium parameter (R_L) indicates the type of isotherm to be irreversible ($R_L = 0$), favorable ($0 < R_L < 1$),

linear (R_L = 1) or unfavorable (linear) (R_L > 1) (Rahman et al., 2010).

According to (Aly et al., 2014), the values of R_L are less than 1 and greater than 0 indicating the favorable sorption Cd^{2+} onto the different adsorbents. While the value of R_L for synthetic zeolite-Y is close to zero (0.019–0.007) as shown in Table 3 and Figure 13 indicating adsorption characteristic is irreversible.

Freundlich adsorption isotherm

The Freundlich expression is a heterogeneous surface-based, analytical equation. Freundlich isotherm can be given by equation (10) (Freundlich & Hatfield, 1926)

$$q_e = k_F C_e^{1/n} \qquad (10)$$

where: q_e (mg/g) is the adsorbed amount of metal ions, $C_{e\ (mg/L)}$ is the equilibrium concentration of metal ions in the solution, K_F is the constants related to the adsorption capacity, n is an empirical parameter related to the intensity of adsorption, which varies with the heterogeneity of the adsorbent. For values in the range $0 < 1/n < 1$, adsorption is favorable; the linear form of the Freundlich isotherm equation (11) is given by:

$$\text{Log } q_e = \log K_F + 1/n \log C_e \qquad (11)$$

Harkins-Jura adsorption isotherm

Harkins-Jura isotherm explains multi-layer adsorption in connection with the presence of a heterogeneous pore distribution and as explained in (Harkins & Jura, 1944), the linear form of the Harkins-Jura isotherm equation (12) is given by:

$$1/q_e^2 = (B/A) - (1/A) \log C_e \qquad (12)$$

where: A and B are the Harkins-Jura constants which are obtained from slope and interception values. Higher B values indicate the higher contribution of physical adsorption.

Adsorption isotherms describe the interaction between Cd^{2+} and porous adsorbents. The parameters obtained from the three isotherm models were represented in Table 4. The comparison between the experimental adsorption results with the isotherm models(Freundlich, Langmuir, and Hrkins- Jura models) on Cd $^{2+}$ ions using SEZ sorbent is illustrated in Figure (13 a, b, and c), respectively.

From this study it can be seen that the value of linear correlation coefficient (R^2) is located in (0.965) demonstrating that the experimental data fitted well with the Langmuir isotherm model on SEZ. The Langmuir maximum sorption capacity Q_m was found at a high value (14.006 g/g) for the SEZ. This result reveals that SEZ has great potential for Cd^{2+} ions removal from contaminated solutions; this finding indicates that the Cd adsorption on the porous adsorbent sample follows the Langmuir monolayer adsorption. As summarized in Table 4.

From the Freundlich isotherm constant can be used to calculate the adsorption capacity and intensity of the reaction and to explore the favorability of a sorption process the values of n lies between one and ten this indicates a favorable sorption process (Dada et al., 2012). From the data in Table 4, the value of $1/n < 1$ indicating that the sorption of Cd^{2+} ions onto the adsorbent is favorable at the studied conditions (Yildiz, 2017; Chen & Shi, 2017). The heterogeneity factor value 1/n near to zero that conform heterogeneous distribution of adsorption sites on the adsorbent surface. The R^2 value is 0.867 for the SEZ. In Harkin-Jura isotherm, R^2 value is closer to unity for the Langmuir isotherm model than that for the Harkins-Jura isotherm models for Cd^{2+} ions adsorption.

k_F and A are the parameters for maximum sorption capacity for the Freundlich and Harkins-Jura equations. From the results the nature of metal ions adsorption on the adsorbent is more compatible with the Langmuir isotherm model; this indicates the occurrence of homogeneous and single-layered adsorption on the used sorbent. The applicability of the three isotherm's models for the present data nearly followed the order: Langmuir > Harkins–Jura > Freundlich.

These results reveal that the Cd^{2+} ions adsorption on SEZ is against the rule of multilayer adsorption (Erdogan, 2019). The sorption capacity followed the trend of CEC values; however, the synthetic zeolite-Y has a high value of CEC (401.09 meq/100g clay) (Singh et al., 2000).

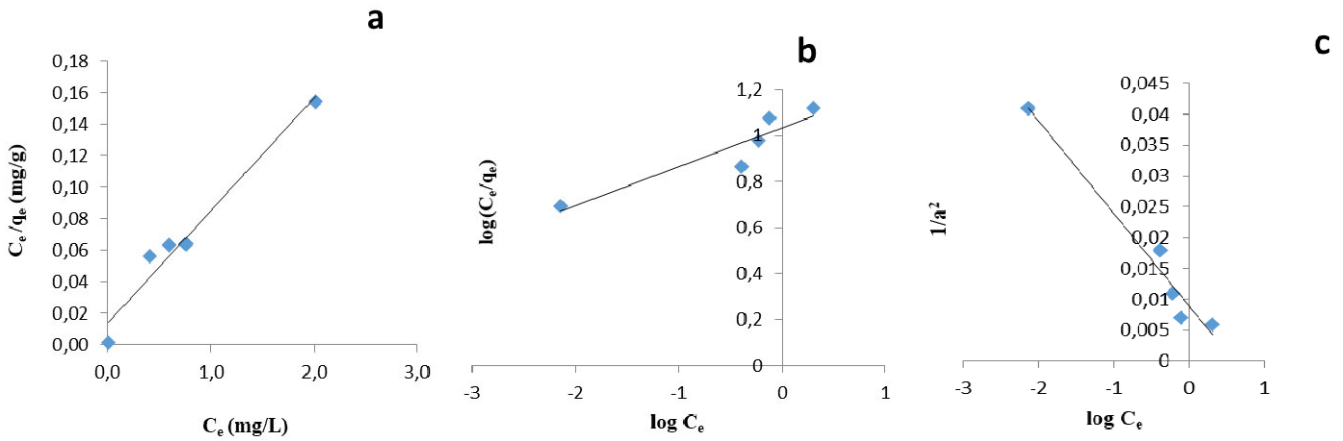

Fig. 13. Linearized Langmuir (a), Freundlich (b) and Harkins-Jura (c) isotherms for the adsorption of Cd^{2+} onto SEZ

According to (Aly et al., 2014), the values of R_L were shown in Figure 14 are less than one and greater than zero indicating the favorable sorption Cd^{2+} onto adsorbent. While the value of R_L for synthetic zeolite-Y is close to zero (0.019–0.007) indicating adsorption characteristic is irreversible.

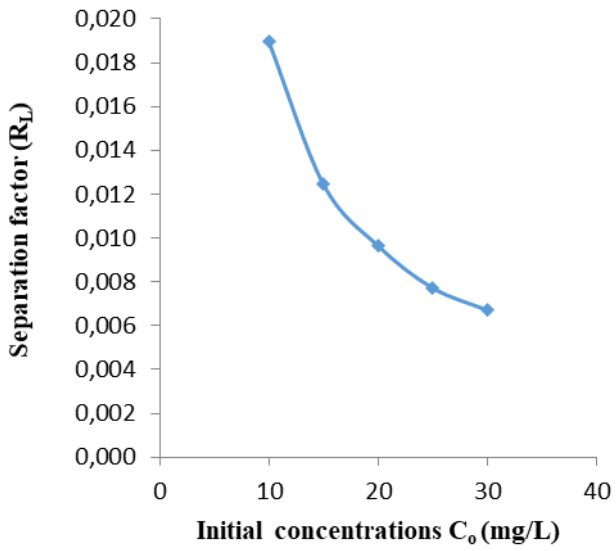

Fig. 14. Separation factor R_L of Cd^{2+} ions onto SEZ

pH changes as a result of metal adsorption

The aqueous solution pH seems to be an important factor for controlling the adsorption mechanism and cadmium ions removal on aluminosilicates (Fahmy et al., 2016). During the sorption experiments, pH in equilibrium solutions was recorded at different initial metal concentrations. This is shown in Figure 15 for Cd^{2+} ions. The figure revealed that the case of synthetic zeolite-Y adsorbent pH increases gradually with an increase in the amount removed. According to (Chen et al., 2011) an increase of the solution pH induces an increase in the adsorption of Cd^{2+} ions, with increasing pH the number of negatively charged: SO^- groups and the hydrolysis of Cd^{2+} ions increases, which leads to an increase of Cd^{2+} ions adsorption.

Table 4

Langmuir, Freundlich and Harkin-Jura isotherm constants for the adsorption of Cd^{2+}ions onto synthetic zeolite-Y.

Parameters	Adsorbent
	Synthetic zeolite-Y
Langmuir isotherm model	
$C/q = C/Q_m + 1/(K_L Q_m)$	y = 0.0714x + 0.0136
Q_m (mg/g)	14.006
K_L(L/mg)	5.25
R_L	0.019 - 0.007
R^2	0.969
Freundlich isotherm model	
$\log q_e = \log K_f + 1/n (\log Ce)$	y = 0.1687x + 1.0322
K_F(L/mg)	10.769
1/n	0.169
n	5.928
R^2	0.867
Harkin-Jura isotherm model	
$1/q_e^2 = B/A - (1/A) \log C_e$	y = - 0.015 x + 0.0089
A	66.67
B	0.593
R^2	0.966

By increasing pH, the number of H^+ ions reduced and then the competition between H^+ ions and metal ions for adsorption sites decreased. Therefore, the adsorption of Cd^{2+} ions into synthetic zeolite-Y increased. Cd^{2+} ions may form complexes with OH^-. However, metal ions have a significant impact on the removal efficiency of zeolite and the selectivity of the metal ions by zeolite was also influenced by the character of metal complex predominating at a common pH value. As known, zeolite has hydroxyl groups which exist on the surface (Si-OH and Al-OH); therefore, degree of ionization depends on the pH values, and the acid/base reaction occurring between the hydroxyl groups on the surface with Cd^{2+} ions from solution (Covarrubias et al., 2005).

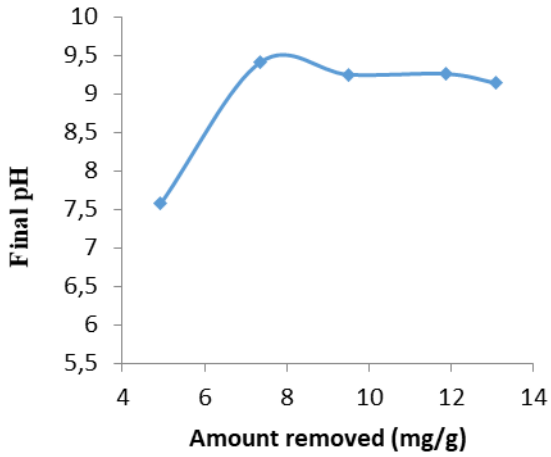

Fig. 15. Relationship between metal sorbbed amount and final pH after 20 min of Cd^{2+} ions interaction with ESZ

4. Conclusions

In this study, batch adsorption experiments for the removal of Cd^{2+} from aqueous solutions were carried out using Egyptian synthetic zeolite-Y from Hagul area as low-cost adsorbents. The adsorption characteristics were examined at initial ion concentrations, contact time initial pH of Cd^{2+} solution, the obtained results can be summarized as follows:

- It was observed that the best time for synthetic zeolite-Y was 10 minutes, in which the substance was saturated with the element and it reached for stability at 20 min and the removal efficiency reached 99.926 %.
- The experimental data were better described by the pseudo-second-order model as evident from the correlation coefficient values (R^2).
- The Langmuir isotherm model was found to be better fitted than the Harkins-Jure and Freundlich isotherm models and the monolayer adsorption capacity for Cd^{2+}onto SEZ was 14.006 mg/g.

Synthetic zeolite-Y can be considered a good alternative adsorbent for removing metal ions from wastewater and contaminated soil immobilization when considering the abundance of low-cost raw materials used for its preparation.

References

Adeoye, J. B., Omoleye, J., Ojewumi, M. E., & Babalola, R. (2017). Synthesis of Zeolite Y from Kaolin Using Novel Method of Dealumination. *International Journal of Applied Engineering Research*, 12(5), 755–760. https://www.ripublication.com/ijaer17/ijaerv12n5_27.pdf.

Ali, M. E. (2018). Synthesis and adsorption properties of chitosan-CDTA-GO nanocomposite for removal of hexavalent chromium from aqueous solutions. *Arabian Journal of Chemistry*, 11(7), 1107–1116. doi: 10.1016/j.arabjc.2016.09.010.

Al-Rudaini, K. A. (2017). Adsorption Removal of Rhodamine-B Dye from Aqueous Solution Using Rhamnus Stone as Low-

Cost Adsorbent. *Al-Nahrain Journal of Science*, 20(1), 32–41. doi: 10.22401/JNUS.20.1.05.

Aly, Z., Graulet, A., Scales, N., & Hanley, T. (2014). Removal of aluminum from aqueous solutions using PAN-based adsorbents: characterization, kinetics, equilibrium and thermodynamic studies. *Environmental Science and Pollution Research*, 21(5), 3972–3986. doi: 10.1007/s11356-013-2305-6.

Aragaw, T. A., & Ayalew, A. A. (2019). Removal of water hardness using zeolite synthesized from Ethiopian kaolin by hydrothermal method. *Water Practice and Technology*, 14(1), 145–159. doi: 10.2166/wpt.2018.116.

Aveen, H. M. & Kafia, M. S. (2014). Kinetics of cation exchange capacity of homoionic sodium form NaY zeolite. *International Journal of Innovative Research in Science, Engineering and Technology,* 3(6), 13137–13137.

Ayoola, A. A., Hymore, F. K., Ojewumi, M. E., & Uwoghiren, O. J. (2018). Effects of Sodium Hydroxide Concentration on Zeolite Y Synthesized from Elefun Kaolinite Clay in Nigeria. *International Journal of Applied Engineering Research*, *13*(3), 1536–1536. http://eprints.covenantuniversity.edu.ng/11144.

Ayoola, A. A., Hymore, F. K., Omodara, O. J., Oyeniyi, E. A., Fayomi, O. S., & Chisom, U. C. (2017). Effect of Crystallisation Time on the Synthesis of Zeolite Y from Elefun Kaolinite Clay. *International Journal of Applied Engineering Research*, 12(21), 10981–10988. https://www.ripublication.com/ijaer17/ijaerv12n21_65.pdf.

Belaabed, R., Elknidri, H., Elkhalfaouy, R., Addaou, A., Laajab, A., & Lahsini, A. (2017). Zeolite Y synthesis without organic template: The effect of synthesis parameters. *J. Mater. Environ. Sci.*, 8, 3550–3555. https://www.jmaterenvironsci.com/Document/vol8/vol8_N10/374-JMES-Belaabed.pdf.

Black, C. A., Evans, D. D., Ensminger, L. E., White, J. L., & Clark, F. E. (1985). Methods of soil analysis. American Society of Agronomy, Inc., Madison, Wisconsin, USA Library of Congress Catalog card Number: 65-15800, U.S.A. 7th printing.

Chen, G., & Shi, L. (2017). Removal of Cd (II) and Pb (II) ions from natural water using a low-cost synthetic mineral: behavior and mechanisms. *RSC advances*, 7(69), 43445–43454. doi: 10.1039/C7RA08018B.

Chen, Y. G., Ye, W. M., Yang, X. M., Deng, F. Y., & He, Y. (2011). Effect of contact time, pH, and ionic strength on Cd (II) adsorption from aqueous solution onto bentonite from Gaomiaozi, China. *Environmental Earth Sciences*, 64(2), 329–336. doi: 10.1007/s12665-010-0850-6.

Covarrubias, C., Arriagada, R., Yanez, J., Garcia, R., Angélica, M., Barros, S. D., & Sousa-Aguiar, E. F. (2005). Removal of chromium (III) from tannery effluents, using a system of packed columns of zeolite and activated carbon. *Journal of Chemical Technology & Biotechnology: International Research in Process, Environmental & Clean Technology*, 80(8), 899–908. doi: 10.1002/jctb.1259.

Dada, A. O., Olalekan, A. P., Olatunya, A. M., & Dada, O. J. I. J. C. (2012). Langmuir, Freundlich, Temkin, and Dubinin–Radushkevich isotherms studies of equilibrium sorption of Zn^{2+} unto phosphoric acid modified rice husk. *IOSR Journal of Applied Chemistry*, *3*(1), 38–45. https://pdfs.semanticscholar.org/9da4/648925199ce9659969c7d3a5fb4e895426a9.pdf.

EL Zayat, M. A. K. (2014). Adsorption of heavy metals cations in wastewater using cement kiln dust. PhD diss., The American University in Cairo.

El-Naggar, I. M., Ahmed, S. A., Shehata, N., Sheneshen, E. S., Fathy, M., & Shehata, A. (2019). A novel approach for the removal of lead (II) ion from wastewater using Kaolinite/Smectite natural composite adsorbent. *Applied Water Science*, 9(1), 7. doi: 10.1007/s13201-018-0845-0.

Erdogan, F. O. (2019). Freundlich, Langmuir, Temkin and Harkins-Jura Isotherms Studies of H_2 Adsorption on Porous Adsorbents. *Chemistry*, *13*(2), 129–135. doi: 10.23939/chcht13.02.129.

Fahmy, A., Youssef, H. F., & Elzaref, A. S. (2016). Adsorption of Cadmium Ions onto Zeolite-A prepared from Egyptian Kaolin using Microwave. *Int J Sci Res*, *5*, 1549–1555.

Fakhri, A. (2017). Adsorption characteristics of graphene oxide as a solid adsorbent for aniline removal from aqueous solutions: Kinetics, thermodynamics and mechanism studies. *Journal of Saudi Chemical Society*, 21(1), S52–S57. doi: 10.1016/j.jscs.2013.10.002.

Fathy, M., Moghny, T. A., Mousa, M. A., El-Bellihi, A. H. A., & Awadallah, A. E. (2016). Absorption of calcium ions on oxidized graphene sheets and study its dynamic behavior by kinetic and isothermal models. *Applied Nanoscience*, *6*(8), 1105–1117. doi: 10.1007/s13204-016-0537-8.

Fatimah, I., & Rubiyanto, D. (2018). Effect of KF Modification to Kaolinite Catalytic Activity in Microwave-Assisted Biodiesel Conversion. *Egyptian Journal of Chemistry*, 61(1), 213–223. doi: 10.21608/ejchem.2018.2041.1163.

Franus, M., Bandura, L., & Madej, J. (2019). Mono and Poly-Cationic Adsorption of Heavy Metals Using Natural Glauconite. *Minerals*, 9(8), 470. doi: 10.3390/min9080470.

Freundlich, H., & Hatfield, H. S. (1926). Colloid and capillary chemistry, Methuen and Co. *Ltd., London*, 110–114.

Guan, L., Wang, Z., & Lu, D. (2019). Evolution of Zeolite Crystals in Self-Supporting Faujasite Blocks: Effects of Hydrothermal Conditions. *Materials*, 12(12), 1965. doi: 10.3390/ma12121965.

Hardie, M., & Doyle, R. (2012). Measuring soil salinity. In *Plant salt tolerance* (pp. 415–425). Humana Press, Totowa, NJ.

Harkins, W. D., & Jura, G. (1944). Surfaces of solids. XIII. A vapor adsorption method for the determination of the area of a solid without the assumption of a molecular area, and the areas occupied by nitrogen and other molecules on the surface of a solid. *Journal of the American Chemical Society*, 66(8), 1366–1373. doi: 10.1021/ja01236a048.

Ho, Y. S., & McKay, G. (1998). A comparison of chemisorption kinetic models applied to pollutant removal on various sorbents. *Transactions of the Institution of Chemical Engineers*, 76(4), 332–340. doi: 10.1205/095758298529696.

Hong, M., Yu, L., Wang, Y., Zhang, J., Chen, Z., Dong, L., & Li, R. (2019). Heavy metal adsorption with zeolites: The role of hierarchical pore architecture. *Chemical Engineering Journal*, 359, 363–372. doi: 10.1016/j.cej.2018.11.087.

Iftitahiyah, V. N., Prasetyoko, D., Nur, H., Bahruji, H., & Hartati, H. (2018). Synthesis and characterization of zeolite NaX from Bangka Belitung Kaolin as alternative precursor. *Malaysian Journal of Fundamental and Applied Sciences*, 14(4), 414–418. doi: 10.11113/mjfas.v14n4.964.

Ismael, I. S., Melegy, A., & Kratochvíl, T. (2012). Lead removal from aqueous solution by natural and pretreated zeolites. *Geotechnical and Geological Engineering*, 30(1), 253–262. doi: 10.1007/s10706-011-9466-1.

Jamil, T. S., Ibrahim, H. S., El-Maksoud, I. A., & El-Wakeel, S. T. (2010). Application of zeolite prepared from Egyptian kaolin for removal of heavy metals: I. Optimum conditions. *Desalination*, 258(1–3), 34–40. doi: 10.1016/j.desal.2010.03.052.

Ji, Z., Su, L., & Pei, Y. (2020). Synthesis and toxic metals (Cd, Pb, and Zn) immobilization properties of drinking water treatment residuals and metakaolin-based geopolymers. *Materials Chemistry and Physics*, 242, 122535.

Khalifah, S. N., Aini, Z. N., Hayati, E. K., Aini, N., & Prasetyo, A. (2018). Synthesis and characterization of mesoporous NaY zeolite from natural Blitar's kaolin. *Materials Science and Engineering*, 333(1), 012005. doi: 10.1088/1757-899X/333/1/012005.

Kwakye-Awuah, B., Sefa-Ntiri, B., Von-Kiti, E., Nkrumah, I., & Williams, C. (2019). Adsorptive Removal of Iron and Manganese from Groundwater Samples in Ghana by Zeolite Y Synthesized from Bauxite and Kaolin. *Water*, 11(9), 1912. doi: 10.3390/w11091912.

Lagergren, S. K. (1898). About the theory of so-called adsorption of soluble substances. *Sven. Vetenskapsakad. Handingarl*, 24, 1–39.

Langmuir, I. (1918). The adsorption of gases on plane surfaces of glass, mica, and platinum. *Journal of the American Chemical Society*, 40(9), 1361–1403. doi: 10.1021/ja02242a004.

Mehdizadeh, S., Sadjadi, S., Ahmadi, S. J., & Outokesh, M. (2014). Removal of heavy metals from aqueous solution using platinum nanoparticles/ Zeolite-4A. *Journal of Environmental Health Science and Engineering*, 12(1), 7. doi: 10.1186/2052-336X-12-7.

Merrikhpour, H., & Jalali, M. (2013). Comparative and competitive adsorption of cadmium, copper, nickel, and lead ions by Iranian natural zeolite. *Clean Technologies and Environmental Policy*, 15(2), 303–316. doi: 10.1007/s10098-012-0522-1.

Mishra, P. C., & Patel, R. K. (2009). Removal of lead and zinc ions from water by low-cost adsorbents. *Journal of Hazardous Materials*, 168(1), 319–325. doi: 10.1016/j.jhazmat.2009.02.026.

Naiya, T. K., Bhattacharya, A. K., & Das, S. K. (2009). Adsorptive removal of Cd (II) ions from aqueous solutions by rice husk ash. *Environmental progress & sustainable energy*, *28*(4), 535–546. doi: 10.1002/ep.10346.

Olaremu, A. G., Odebunmi, E. O., Nwosu, F. O., Adeola, A. O., & Abayomi, T. G. (2018). Synthesis of zeolite from kaolin clay from Erusu Akoko southwestern. *Journal of Chemical Society of Nigeria*, 43(3), 381–786. http://journals.chemsociety.org.ng/index.php/jcsn/article/view/188.

Ören, A. H., & Kaya, A. (2006). Factors affecting adsorption characteristics of Zn2+ on two natural zeolites. *Journal of hazardous materials*, 131(1-3), 59–65. doi: 10.1016/j.jhazmat.2005.09.027.

Rahimi, M., & Mahmoudi, J. (2020). Heavy Metals Removal from Aqueous Solution by Modified Natural Zeolites Using Central Composite Design. *Periodica Polytechnica Chemical Engineering*, 64(1), 106–115. doi: 10.3311/PPch.13093.

Rahman, A. U., Khan, F. U., Rehman, W. U., & Saleem, S. (2018). Synthesis and characterization of zeolite 4A using swat kaolin. *Journal of Chemical Technology and Metallurgy*, 53(5), 825–829. https://dl.uctm.edu/journal/node/j2018-5/5_17-121_p825-829.pdf.

Rahman, R. A., Ibrahim, H. A., Hanafy, M., & Monem, N. A. (2010). Assessment of synthetic zeolite Na A–X as a sorbing barrier for strontium in a radioactive disposal facility. *Chemical Engineering Journal*, 157(1), 100–112. doi: 10.1016/j.cej.2009.10.057.

Rani, R. D., & Sasidhar, P. (2012). Sorption of cesium on clay colloids: kinetic and thermodynamic studies. *Aquatic geochemistry*, 18(4), 281–296. doi: 10.1007/s10498-012-9163-6.

Shaheen, S. M., Derbalah, A. S., & Moghanm, F. S. (2012). Removal of heavy metals from aqueous solution by zeolite in competitive sorption system. *International Journal of Environmental Science and Development*, 3(4), 362. http://www.ijesd.org/papers/248-CD0058.pdf.

Singh, B., Alloway, B. J., & Bochereau, F. J. M. (2000). Cadmium sorption behavior of natural and synthetic zeolites. *Communications in soil science and plant analysis*, 31(17–18), 2775–2786. doi: 10.1080/00103620009370626.

Somderama, S., Aziza, A. S. A., Abdullaha, A. H., & Matb, R. (2019). Characterisation of NaA Zeolite Made from Malaysian Kaolin. *Chemical Engineering*, 72. doi: 10.3303/CET1972055.

Tavasoli, M., Kazemian, H., Sadjadi, S., & Tamizifar, M. (2014). Synthesis and characterization of zeolite NaY using kaolin with different synthesis methods. *Clays and Clay Minerals*, 62(6), 508–518. doi: 10.1346/CCMN.2014.0620605.

Warzybok, M., & Warchol, J. (2018). Synthesis of kaolin-based zeolite Y and its application for adsorption of two carbonyl compound gases. *Czasopismo Inżynierii Lądowej, Środowiska i Architektury*, 65, 13–26. doi: 10.7862%2Frb.2018.2.

Yildiz, S. (2017). Kinetic and isotherm analysis of Cu (II) adsorption onto almond shell (Prunus dulcis). *Ecological Chemistry and Engineering S*, 24(1), 87–106. doi: 10.1515/eces-2017-0007.

Yuna, Z. (2016). Review of the natural, modified, and synthetic zeolites for heavy metals removal from wastewater. *Environmental Engineering Science*, 33(7), 443–454. doi: 10.1089/ees.2015.0166.

Yusof, Y., Sugimoto, K., Ozawa, H., Uno, S., & Nakazato, K. (2010). On-chip microelectrode capacitance measurement for biosensing applications. *Japanese Journal of Applied Physics*, 49(1S), 01AG05. doi: 10.1143/JJAP.49.01AG05.

Zewail, T. M., & Yousef, N. S. (2015). Kinetic study of heavy metal ions removal by ion exchange in batch conical air spouted bed. *Alexandria Engineering Journal*, 54(1), 83–90. doi: 10.1016/j.aej.2014.11.008.